Energy renormalization and Mott transition in n-GaAs and n-GaN

P. N. Romanets* and A. V. Sachenko

In this paper, we investigate renormalization of charge carrier effective masses and bandgap narrowing in n-GaAs and wurtzite-type n-GaN over a wide range of temperatures and dopant concentrations. The calculations are based on the Green's function formalism. Contrary to the previous works, we consider the regions below as well as above the Mott transition. Special attention is paid to formation of donor subband and condition for the Mott transition. We also take into account the effects caused by optical phonons. The latter strongly depend on the doping level because of dynamic screening. It is shown that three specific doping levels may be set off in n-GaN. They correspond to 1) Mott transition, 2) resonance amplification of optical phonon-plasmon, and 3) full dynamic screening of optical phonons, respectively. Contrary to the case of n-GaN, the effect of full dynamic screening cannot be implemented in n-GaAs because of stronger nonparabolicity of conduction band.

* pn_romanets@yahoo.com

I. INTRODUCTION

To date, practical interest in heavily doped semiconductors remains at a high level. The improved technology created opportunities for high-quality semiconductor samples making with, specified concentrations of the major and compensating impurities. The role of other types of defects can be minimized by varying the temperature of the substrate, growth temperature and annealing of the samples [1–3].

The temperature characteristics of semiconductor devices are often decisive in determining their applicability. This in turn determines high interest in the electronic properties of semiconductors near the Mott transition [4]. The study of metal-semiconductor Mott transition has a deep history. Back in 1948, the work by Pearson and Bardeen showed that, at high levels of silicon doping, its current-voltage characteristics become ohmic and the Hall coefficient is independent of temperature [5]. Delimitation of the transition is especially important for new materials as non-monotonic temperature dependence of the Hall coefficient near the transition can lead to incorrect interpretation of experimental data [6, 7]. An accurate calculation of the temperature dependence of the electron concentration also allows to independently determine the Hall scattering factor. Given the importance of the Mott transition to semiconductor technology the investigation is relevant today [7–10].

In the present work, we propose a detailed theoretical analysis of renormalization of the charge carrier effective masses and bandgap narrowing in n-GaAs and n-GaN over a wide range of temperatures and doping levels. That is essential in the study of interband transitions, and especially for the excitonic processes. We emphasize on the electronic properties of the semiconductors near the metal-semiconductor Mott transition. The latter appears when screening length is about 17% lower than the Bohr radius of shallow donors.

The paper is organized in the following way. In the first section we derive equation for dispersion law of donor subband. In the second section we discuss applied the Green's function approach. In the third section we introduce the closed set of equations for unknown parameters (screening length, effective mass and chemical potential). The results of computation and their analysis are presented in third section. In Conclusions, we discuss the approaches used and summarize the results obtained.

II. DONOR SUBBAND

Shallow donor level can be described by a Hamiltonian [11–13]:

$$\hat{H} = \frac{\hat{\mathbf{p}}^2}{2m} - \frac{e^2}{\epsilon r}\exp(-\lambda r), \tag{1}$$

here λ^{-1} is the screening length e is the elementary charge, ϵ is dielectric constant and m is the renormalized electron effective mass (see next section). The above model of static screening is not valid for $\lambda^{-1} \lesssim r_{B0} = \hbar^2\epsilon/me^2$, but in this case the subband disappears (see below). An exact solution of the Schrödinger equation with Hamiltonian (1) is too complicated for our applications. We use the following approach: application of perturbation theory in the form [11] $\hat{H} = \hat{H}_0 + V$, where $\hat{H}_0 = \hat{\mathbf{p}}^2/2m - e^2/\epsilon r$ and $V = (e^2/\epsilon r)[1 - \exp(-\lambda r)]$. Then we can calculate the first correction to ground state energy $(\hat{H}_0 + V)\Psi \simeq (E_0 + E_1)\Psi$; where $E_0 = -me^4/2\hbar^2\epsilon^2 = -\hbar^2/2mr_{B0}^2$ and $E_1 = (me^4/\hbar^2\epsilon^2)[1 - 4(r_{B0}\lambda + 2)^{-2}]$. Therefore, we can introduce donor ionization energy $E_{d0} = E_0 + E_1$:

$$E_{d0} = \frac{\hbar^2}{2mr_{B0}^2}[1 - 8(r_{B0}\lambda + 2)^{-2}], \tag{2}$$

which implies that the subband exists only for $\lambda r_{B0} < 2(\sqrt{2} - 1) \sim 0.8$.

Since the full set of eigenfunctions of (1) is not known, the correction to the wave function $\Psi = \Psi_0 + \Psi_1$ can not be found within the perturbation theory. Therefore, we choose a model wave function as $\Psi = \exp(-r/r_B)/\pi r_B^3$ with a free parameter r_B. The function satisfies the condition for quantum-mechanical average [11]:

$$\int d^3r \Psi^* \hat{H} \Psi = E_{d0}. \tag{3}$$

Thus equations (2) and (3) with the above model Ψ are equivalent to the algebraic equation for λr_B. Overlapping of the donor wave functions leads to a broadening of levels. The donor system can be considered as a weakly ordered sublattice [14, 15]. According to the strong coupling approach (see, for example, Sec. 4.7 in Ref. 16):

$$E_d = E_{d0} + \frac{\sum_{\mathbf{kr}_n>0}\langle 0|U(|\mathbf{r} - \mathbf{r}_n|)|n\rangle \exp(i\mathbf{kr}_n) + h.c.}{\langle 0|0\rangle + \left[\sum_{\mathbf{kr}_n>0}\langle 0|n\rangle \exp(i\mathbf{kr}_n) + h.c.\right]}, \tag{4}$$

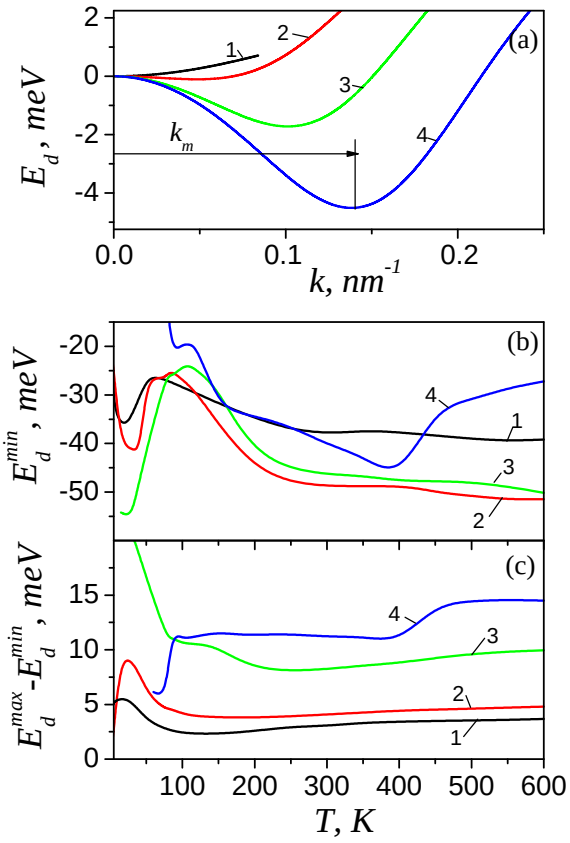

FIG. 1. (a) Energy dispersion law for subband electrons line 1 – $N_d = 10^{16}$ cm^{-3}, 2 – $N_d = 5 \times 10^{16}$ cm^{-3},3 – $N_d = 1.2 \times 10^{17}$ cm^{-3},4 – $N_d = 3 \times 10^{16}$ cm^{-3}, T=77 K; (b) the bottom of the subband measured from the bottom of the conduction band, line 1 – $N_d = 5 \times 10^{16}$ cm^{-3}, 2 – $N_d = 1.2 \times 10^{17}$ cm^{-3},3 – $N_d = 7 \times 10^{17}$ cm^{-3},4 – $N_d = 10^{18}$ cm^{-3}; (c) the subband width lines 1–4 correspond to the same concentrations as in (b).

where $\mathbf{r}_n$ defines the position of the n-th donor, $U(\mathbf{r}) = e^2 \exp(-\lambda r)/\epsilon r$ and E_{d0} is given by eq. (2). The main contribution to the overlap integrals comes from the region near the preferred axis for two neighboring donors. The corresponding expansion in the cosine of the angle in the integrand and replacing the sum with integral allow to obtain an analytic expression for the energy

$$E_d = E_{d0} + \frac{16\pi N_d \frac{e^2}{\epsilon r_B^2}\left[\frac{2r_B^3}{\lambda(1+r_B^2k^2)} - \frac{r_B^2}{\lambda^2(1+r_B^2k^2)} + \frac{\lambda^{-2}+r_B^2(\lambda r_B^2+2)^{-2}}{(\lambda r_B^2+1)^2 r_B^{-2}+k^2}\right]}{1 + 16\pi N_d r_B^3\left[\frac{1}{2(1+r_B^2k^2)} + \frac{1}{4(1+r_B^2k^2)} + \frac{4(1-r_B^2k^2)}{(1+r_B^2k^2)^4}\right]}. \quad (5)$$

Obviously, this dispersion law is valid for finite $k < k_{max}$ only. The cutoff parameter k_{max} is similar to the first Brillouin zone border

$$N_d = \frac{1}{2\pi^2}\int_0^{k_{max}} dk k^2. \quad (6)$$

One can see the energy dispersion law GaN subband electrons in Fig. 1 (a). The calculation was performed for different doping levels $N_d = 5 \times 10^{16}$–10^{18} cm^{-3} and liquid nitrogen temperature. For the peculiarities of screening length λ^{-1} calculation see next sections. The low doping levels (line 1) correspond to the near parabolic dispersion law with minimum energy in the center $E_d^{min} = E_d(0)$ (case i). The higher dopant concentrations (lines 2–4) correspond to the wider subbands with $E_d^{min} = E_d(k_m \neq 0)$ (case ii). Fig. 1 (b) demonstrates how bottom of the subband E_d^{min} depends on temperature and doping level. Similarly, the Fig. 1 (c) demonstrates how subband width depends on temperature and doping level.

III. EFFECTIVE MASS RENORMALIZATION AND BANDGAP NARROWING

Accurate consideration of the Mott transition requires taking into account the effects of renormalization. Indeed, states filling in the conduction band and the donor subband depends on the density of states. The latter is modified at high doping levels due to the effective mass renormalization and departure time decreasing. We also perform calculation of the bandgap narrowing to compare our results with the previous calculation and experimental data. One should consider, at least, the exchange interaction, electron-impurity, electron-electron and electron-optical phonon interactions to calculate renormalization of the effective mass and lowering the bottom of the conduction band. It is also necessary to take into account the corresponding interaction mechanisms for heavy holes to calculate rise of the valence band top owing to energy renormalization. The same effect for light holes is somewhat lower. Some interesting effects originating from dynamic screening of optical phonons [17] is also considered below.

Our calculations are based on the Green's functions formalism and are generally very similar to the calculation performed in Ref. 18, 19 (for fundamental theory see, e. g., Ref. 22, pp. 107-113). For this reason, we present only the basic formulas. We also will pay more attention to the points that differ significantly from the above-mentioned works. The aim of these differences will be associated with an attempt to improve the accuracy of calculations.

For more generality, we start with many particle Green's function

$$G_E(1,2,..,n;1',2',..,n') = \sum_\gamma \frac{|1,2,..,n\rangle_\gamma \langle 1',2',..,n'|_\gamma}{E - E_\gamma - io}. \tag{7}$$

The vectors in the right-hand side include all permutations (Slater determinant). The self-energy function is defined through averaged Green's functions The self-energy function is defined through averaged Green's functions

$$\begin{array}{l} \Sigma^\alpha = \sum_\beta \Sigma^{\alpha\beta}_{HF} + \left\langle \sum_{\Delta\mathbf{p}} \frac{|\langle \mathbf{p}_1|_\alpha V_d |\mathbf{p}_1+\Delta\mathbf{p}\rangle_\alpha|^2}{E-E_{\mathbf{p}_1+\Delta\mathbf{p},\mathbf{p}_2}-io} + \right. \\ \left. \sum_{\Delta\mathbf{p}} \frac{|\langle \mathbf{p}_1|_\alpha V_{opt} |\mathbf{p}_1+\Delta\mathbf{p}\rangle_\alpha|^2}{E-E_{\mathbf{p}_1+\Delta\mathbf{p},\mathbf{p}_2}\pm\hbar\omega_o-io}(N_{\hbar\omega_o/T} + \frac{1}{2} \pm \frac{1}{2}) + \sum_{\beta\Delta\mathbf{p}} \frac{|\langle \mathbf{p}_1|_\alpha \langle \mathbf{p}_2,..,\mathbf{p}_n|_\beta V_{\alpha\beta} |\mathbf{p}_2-\Delta\mathbf{p},..,\mathbf{p}_n\rangle_\beta |\mathbf{p}_1+\Delta\mathbf{p}\rangle_\alpha|^2}{E-E_{\mathbf{p}_1+\Delta\mathbf{p},\mathbf{p}_2-\Delta\mathbf{p},..}-io} + ... \right\rangle , \end{array} \tag{8}$$

where index $\alpha = e, lh, hh$ corresponds to electrons or light (heavy) holes and $\beta = e, se$ corresponds to conduction band or donor subband electrons. The first term is self-energy due to exchange interaction in the Hartree—Fock approach. The interparticle interactions are described by operators $V_{\alpha\beta}$, the particle-impurity and particle-optical phonon interactions are described by V_d and V_{opt} ($\hbar\omega_o$is the optical phonon energy and $N_{\hbar\omega_o/T}$ is the Planck distribution). We would like to emphasize that donor subband appears only in some range of dopant concentration below the Mott transition. We omit higher order terms and the term that disappears due to averaging. The averaging supposes both impurity ensemble and electron ensemble averaging.

Most experiments on bandgap narrowing in GaAs are performed for donor concentration up to 10^{20} cm^{-3}. At such doping levels the effect of nonparabolicity is essential over the whole temperature range. For this reason we use the energy dispersion law in relativistic form $\varepsilon(p) = p_s^2(\sqrt{1 + p^2/p_s^2} - 1)/m$, where $p_s \simeq \sqrt{mE_g/2}$, $\mathbf{p}$ is the electron momentum, E_g is the low concentration bandgap and m is the renormalized electron effective mass. Nonparabolicity is not essential for valence holes but may be of essence for subband electrons than we also use the same dispersion law and determine p_{sse}, m_{se} from (5).

There are two ways to improve our calculation accuracy. One of them is to take into account the higher order terms in (8), while another is to start from the Green's function that already contains self-energy rather than from the Green's function of non-interacting system of free electrons. Here we used the second approach. First, we obtain imaginary part of the self-energy using screened potential as in eq. (1). Considering two interacting charged particles and neglecting the terms of order $(\lambda\hbar/p_s)^2 << 1$ (the condition is adequate because $\lambda\hbar$ is much lower than Fermi momentum at high doping levels) one can obtain the following expression for the probability W of transition from the states $\mathbf{p}_1$, $\mathbf{p}_2$ to states $\mathbf{p}_1'$, $\mathbf{p}_2' = \mathbf{p}_1 - \mathbf{p}_1' + \mathbf{p}_2$ per unit time:

$$\hbar \cdot W(\mathbf{p}_1', \mathbf{p}_2', \mathbf{p}_2) = \frac{8\pi N_{\mathbf{p}_2}(e^2/\epsilon)^2 \widetilde{m}_r}{\lambda^3 \hbar^2} \frac{v_r/v_\lambda}{4(v_r/v_\lambda)^2 + 1}. \tag{9}$$

where $v_r = |\mathbf{p}_1'/\widetilde{m}_1 - \mathbf{p}_2'/\widetilde{m}_2|$ with $\widetilde{m}_{1,2} = m_{1,2}\sqrt{1 + (p'_{1,2}/p_{s1,2})^2}$ and $\widetilde{m}_r = [\widetilde{m}_1^{-1}/(1 + p'^2_1/p^2_{s1})^{3/2} + \widetilde{m}_2^{-1}/(1 + p'^2_2/p^2_{s2})^{3/2}]^{-1}$. The latter is effective reduced mass when $p_{1,2} << p_{s1,2}$. Also we introduce characteristic velocity $v_\lambda = \lambda\hbar/\widetilde{m}_r$ and $N_{\mathbf{p}_2}$ is the concentration of the particles with momentum $\mathbf{p}_2$. Using the limiting transition $m_2 \longrightarrow \infty$ in eq. (9) we obtain self-energy imaginary part due to interaction with donors ($m_1 = m_{lh,hh,e}$). One can obtain imaginary part due to interaction with the conduction band or subband electrons by substituting $\mathbf{p}'_{1,2} = \mathbf{p}_{1,2} \pm \Delta\mathbf{p}$

and then performing averaging over $\mathbf{p}_2$. We use zero temperature approach to obtain analytic form

$$\varepsilon_{12}^{im} \simeq \frac{(e^2/\epsilon)^2\widetilde{m}_2^3}{4\pi\hbar^2\widetilde{m}_r^2}\begin{cases} -\frac{b_f^2+1-a^2}{2a}[\arctan(b_f+a)+\arctan(b_f-a)]+ \\ \frac{2b_f^3}{3a}+\frac{b_f}{a}-\frac{1}{2}\ln\{[(b_f+a)^2+1][(b_f-a)^2+1]\}, & b_f<a; \\ 1-\frac{b_f^2+1-a^2}{2a}[\arctan(b_f+a)-\arctan(b_f-a)]+ \\ b_f^2-\frac{a^2}{3}-\frac{1}{2}\ln\{[(b_f+a)^2+1][(b_f-a)^2+1]\}, & b_f>a. \end{cases} \tag{10}$$

where $a=2|\mathbf{p}_1/\widetilde{m}_1+\Delta\mathbf{p}/\widetilde{m}_r|/v_\lambda$ and $b_f=2p_{F2}/\widetilde{m}_2v_\lambda$ (in $\widetilde{m}_r$ p_2 is replaced with p_{F2}). The Fermi momentum is defined by the particles concentration $p_{F2}=\pi^{2/3}\hbar(3N_2)^{1/3}$. We neglect dynamic screening in eqs. (9)-(10) supposing that $\Omega_p\hbar >> \varepsilon^{im}$ for all essential transition (Ω_p is the plasmon frequency).

The electron-optical phonon interaction seems to be independent of the doping level. On the other hand, dynamic screening modifies the field induced by optical phonon. Below we consider such effects. For generality we start from the imaginary part of self-energy induced by optical phonon:

$$\varepsilon_{opt}^{im} \simeq B^{\pm}(p)\begin{cases} |\epsilon_e^{-1}(q_1^{\pm},\omega_o)|^2\ln\left(\frac{q_2^{\pm}}{q_1^{\pm}}\right), & \varepsilon^{im}<\omega_o\hbar/2, \\ \frac{1}{2}\left[\ln\left(\frac{\lambda^2+q_2^{\pm\,2}}{\lambda^2+q_1^{\pm\,2}}\right)+\left(\frac{\lambda^2}{\lambda^2+q_2^{\pm\,2}}-\frac{\lambda^2}{\lambda^2+q_1^{\pm\,2}}\right)\right], & \varepsilon^{im}>\omega_o\hbar/2; \end{cases} \tag{11}$$

where $B^{\pm}(p)=me^2\omega_o(\sqrt{1+(p/p_s)^2}\pm m\hbar\omega_o/p_s^2)(N_{\hbar\omega_o/T}+1/2\pm1/2)/\bar{\epsilon}p$, $\hbar\omega_o$ is the optical phonon energy, $N_{\hbar\omega_o/T}$ is the Planck distribution function, $\bar{\epsilon}^{-1}=\epsilon_\infty^{-1}-\epsilon^{-1}$ is the effective dielectric constant, $q_j^{\pm}(p)=|p+(-1)^j\ \{[\sqrt{1+(p/p_s)^2}\pm m\hbar\omega_o/p_s^2]^2-p_s^2\}^{0.5}\Big|$ and $\varepsilon^{im}(\mathbf{p},\hbar\mathbf{q})\equiv\hbar/2\tau_d=\varepsilon_d^{im}(\mathbf{p}+\hbar\mathbf{q})+\varepsilon_{12}^{im}(\mathbf{p},\hbar\mathbf{q})+\varepsilon_{opt}^{im}(\mathbf{p}+\hbar\mathbf{q})$ [$\epsilon_e(q,\omega)$ is defined in appendix]. The generation of optical phonon is forbidden if $\varepsilon(p)<\hbar\omega_o$ then one has to put $B^-(p)=0$ for this case.

The denominator of last term in eq. (8) includes energy difference of particle 2: $\varepsilon(\mathbf{p}_2)-\varepsilon(\mathbf{p}_2-\Delta\mathbf{p})$. This item makes averaging procedure very complicated. Therefore, we replace it with $\langle\varepsilon(\mathbf{p}_2)-\varepsilon(\mathbf{p}_2-\Delta\mathbf{p})\rangle$. By performing averaging in the same way as for the imaginary part one can obtain:

$$\langle\varepsilon(\mathbf{p}_2)\rangle=-\varepsilon_0\left[\ln\frac{|1+s|}{|1-s|}+\frac{2s}{1-s^2}-\frac{4s}{(1-s^2)^2}\right];$$

$$\langle\varepsilon(\mathbf{p}_2-\Delta\mathbf{p})\rangle=\frac{\varepsilon_0}{2}\sum_{\pm}\left\{\pm\frac{16p_{s2}}{15\Delta p}\left[1+\frac{(p_{F2}\pm\Delta p)^2}{p_{s2}^2}\right]^{2.5}-\left[\ln\left|\frac{1+s_\pm}{1-s_\pm}\right|+\frac{2s_\pm}{1-s_\pm^2}+\frac{4s_\pm}{3(1-s_\pm^2)^2}\right]\right\}; \tag{12}$$

here summation is done over the upper and lower signs $\pm$, and we introduced the values $\varepsilon_0=p_{s2}^5/(16\pi^2\hbar^3m_2N_2)$, $s_\pm=\sin[\arctan(p_{F2}/p_{s2}\pm\Delta p/p_{s2})]$ and $s=\sin[\arctan(p_{F2}/p_{s2})]$. The items described by eqs. (10)-(12) reduce the self-energy [see (8)]. The density of states is modified due to departure time decreasing [22] and effective mass renormalization. The first effect is too complicated and needs special investigation. The rest of effects may be described by the usual formula:

$$\rho(\varepsilon)\simeq\frac{8\sqrt{2}m^{3/2}\pi\sqrt{\varepsilon}\sqrt{1+m\varepsilon/2p_s^2}(1+m\varepsilon/p_s^2)}{(2\pi\hbar)^3}. \tag{13}$$

Below we introduce real parts of self-energy due to exchange interaction in Hartree—Fock approach and due to the electron-optical phonon interaction.

Usually, $\Sigma_{HF}^{\alpha\beta}$ is calculated in zero temperature limit, without nonparabolicity and finiteness of departure time effects. More careful procedure leads to the next formula

$$\Sigma_{HF}^{(e,lh)\beta}(\mathbf{p})=\mp\frac{\pi e^2}{\epsilon}\int_0^\infty d\varepsilon\rho^\beta(\varepsilon)F_\varepsilon^\beta\int_{-1}^1 d\chi\frac{1}{\epsilon_e[q(\chi,\varepsilon,p),0]q^2(\chi,\varepsilon,p)}, \tag{14}$$

where $q^2(\chi,\varepsilon,p)=(p^2+p_\varepsilon^2-2pp_\varepsilon\chi)/\hbar^2$ and $\epsilon_e(q,\omega)$ is defined in appendix A. Notice, the upper sign is correct for electron-electron and conduction band-subband electron exchange interaction. The lower sign stands for light (heavy) hole-subband electron and light (heavy) hole-conduction band electron exchange interaction. If the test particle interacts with electrons ($\beta=e$) then F_ε stands for Fermi function and $\rho(\varepsilon)$ is defined by eq. (13). If the test particle interacts with subband electrons ($\beta=se$) then one has to replace $d\varepsilon\rho F_\varepsilon$ by $dkk^2F_{E_d(k)}/\pi^2$ and $p(\varepsilon)$ by $\hbar k$. The energy $E_d(k)$ is defined by eq. (5).

Finally, we introduce the real part of self-energy induced by optical phonon

$$\Sigma_{opt}^{(e,lh)}(\mathbf{p})=\frac{e^2\hbar\omega_o}{4\bar{\epsilon}\pi^2}\Re\int_\Gamma\frac{d^3\mathbf{q}}{q^2|\epsilon_e(q,\omega_o)|^2}\frac{N_{\hbar\omega_o/T}+\frac{1}{2}\pm\frac{1}{2}}{\varepsilon(\mathbf{p})-\varepsilon(\mathbf{p}+\hbar\mathbf{q})\pm\hbar\omega_o-i\varepsilon^{im}(\mathbf{p},\hbar\mathbf{q})}, \tag{15}$$

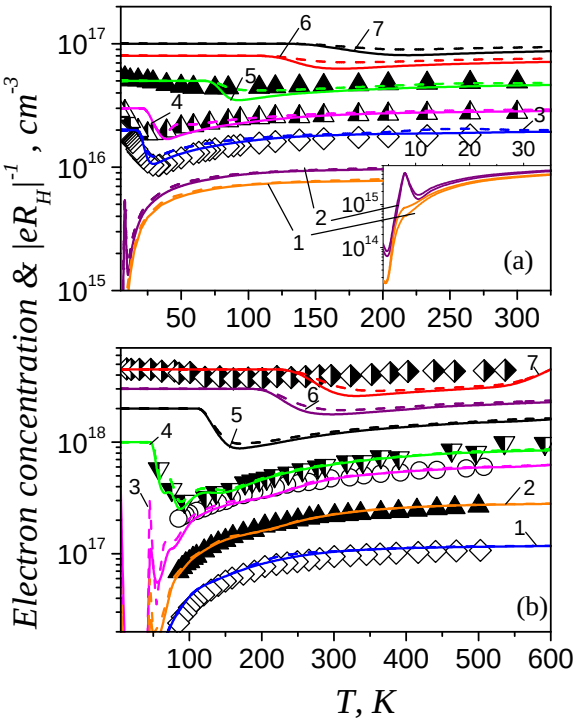

FIG. 2. The conduction band electrons concentrations and inverse Hall coefficients $|eR_H|^{-1}$ as functions of temperature. Calculation was performed for different doping levels. Solid lines is the concentration, dashed is $|eR_H|^{-1}$. (a) GaAs, line 1 – $N_d = 8\times10^{15}\ cm^{-3}$, 2 – $N_d = 10^{16}\ cm^{-3}$, 3 – $N_d = 2\times10^{16}\ cm^{-3}$, 4 – $N_d = 3\times10^{16}\ cm^{-3}$, 5 – $N_d = 5\times10^{16}\ cm^{-3}$, 6 – $N_d = 8\times10^{16}\ cm^{-3}$, 7 – $N_d = 10^{17}\ cm^{-3}$ (experimental data sets are extracted from Ref. 2 pg. 41 Fig. 21 and Ref. 3 pg. 103 Fig. 2.18); Inset: lines 1 and 2 in low temperature region; (b) GaN, lines 1 – $N_d = 1.2\times10^{17}\ cm^{-3}$, 2 – $N_d = 3\times10^{17}\ cm^{-3}$, 3 – $N_d = 7\times10^{17}\ cm^{-3}$, 4 – $N_d = 10^{18}\ cm^{-3}$,5 – $N_d = 2\times10^{18}\ cm^{-3}$, 5 – $N_d = 3\times10^{18}\ cm^{-3}$, 6 – $N_d = 4.5\times10^{18}\ cm^{-3}$, (the three bottom experimental data sets are extracted from Ref. 7, and two upper experimental data sets are extracted from Ref. 9).

where $\varepsilon^{im}(\mathbf{p},\hbar\mathbf{q}) = \varepsilon^{im}_{d}(\mathbf{p}+\hbar\mathbf{q}) + \varepsilon^{im}_{12}(\mathbf{p},\hbar\mathbf{q}) + \varepsilon^{im}_{opt}(\mathbf{p}+\hbar\mathbf{q})$. Other designations the same as in eqs. (8), (11). Notice, that the integral is logarithmically divergent. Therefore, we integrate over the finite region $\Gamma : q < 2p_s/\hbar$. The other points of our calculation of self-energy are rather standard and we omit their discussion.

IV. CLOSED SET OF EQUATIONS

To obtain the closed set of equations we have to fulfill introduced below equations with formulas for screening length λ^{-1}, chemical potential μ and renormalized effective mass m. We define inverse screening length from the classical formula:

$$\lambda^2 = \frac{4\pi e^2}{\epsilon}\frac{\partial}{\partial\mu}\begin{cases} \int_0^\infty d\varepsilon \frac{\rho(\varepsilon)}{\exp\left(\frac{\varepsilon-\mu}{T}\right)+1} + \int_0^{k_{max}} \frac{dkk^2}{\pi^2}\frac{1}{\exp\left[\frac{E_d(k)-\mu}{T}\right]+1}, & \frac{\lambda r_{B0}}{\sqrt{2}-1} < 2; \\ \int_0^\infty d\varepsilon \frac{\rho(\varepsilon)}{\exp\left(\frac{\varepsilon-\mu}{T}\right)+1}, & \frac{\lambda r_{B0}}{\sqrt{2}-1} \geq 2; \end{cases} \tag{16}$$

where $E_d(k)$ is defined by eq.(5) and T is the temperature in ergs. The eq. (16) is not exactly valid for low temperature limit or under extremely high doping levels. Nevertheless, for simplicity we extrapolate it to all the parameters considered. To check the validity of (16) we examine the condition $\lambda^{-1} >> a$ (a is the lattice constant).

The full energy of the particle for low momentum values $p << p_s$ is $p^2/2m_{\alpha 0} + \Sigma^\alpha(p) \simeq p^2/2m_\alpha$. Therefore, the renormalized effective mass m_α satisfies the equation:

$$m_\alpha^{-1} = m_{\alpha 0}^{-1} + \left.\frac{\partial^2\Sigma^\alpha(p)}{\partial p^2}\right|_{p=0}; \tag{17}$$

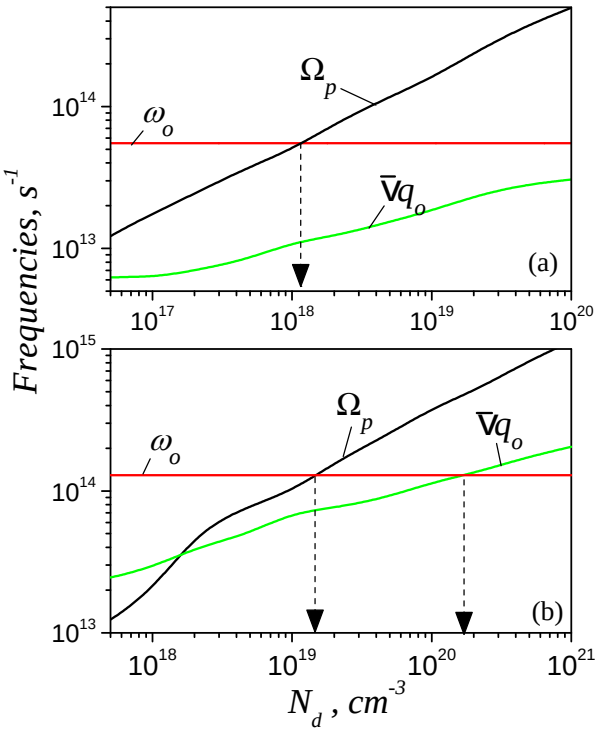

FIG. 3. The frequencies that are relevant to dynamic screening of optical phonon. The optical phonon frequency is ω_o, the plasmon frequency is Ω_p and the frequency of full dynamic screening $\overline{v}q_o$. Here $\varepsilon(\hbar q_o) = \hbar\omega_o$ and $\overline{v}$ is about Fermi velocity and defined in Appendix A. (a) is for GaAs and (b) is for GaN

here $\alpha = e, lh, hh$ and $\Sigma^{\alpha}(p)$ is described in previous section.

The chemical potential μ is satisfies the condition of electroneutrality:

$$N_d = \begin{cases} \int_0^{\infty} d\varepsilon \frac{\rho(\varepsilon)}{\exp\left(\frac{\varepsilon-\mu}{T}\right)+1} + \int_0^{k_{max}} \frac{dkk^2}{\pi^2} \frac{1}{\exp\left[\frac{E_d(k)-\mu}{T}\right]+1}, & \frac{\lambda r_{B0}}{\sqrt{2}-1} < 2; \\ \int_0^{\infty} d\varepsilon \frac{\rho(\varepsilon)}{\exp\left(\frac{\varepsilon-\mu}{T}\right)+1}, & \frac{\lambda r_{B0}}{\sqrt{2}-1} \geq 2; \end{cases} \tag{18}$$

here N_d is the dopant concentration. The eq. (8) for $\Sigma^e(p)$ and eqs. (16)–(18) is the closed set of equations for λ, μ and $m \equiv m_e$. We use numerical-iterative procedure based on Newton method to solve the problem.

To carefully describe Hall effect measurements one has take into account both conduction band and donor subband transport. Supposing that relaxation times is about departure time and Hall scattering factor $r_H \simeq 1$ we estimate Hall coefficient as

$$R_H \simeq -\frac{\left[\frac{N_e}{(\widetilde{m}_e\varepsilon_e^{im})^2} + \frac{N_{se}}{(\widetilde{m}_{se}\varepsilon_{se}^{im})^2}\right]}{|e|\left(\frac{N_e}{\widetilde{m}_e\varepsilon_e^{im}} + \frac{N_{se}}{\widetilde{m}_{se}\varepsilon_{se}^{im}}\right)^2}, \tag{19}$$

here $\varepsilon_{e,se}^{im}$ is the imaginary part of the energy of the subband or conduction band electrons, $N_{e,se}$ are the corresponding concentrations and masses $\widetilde{m}_{e,se}$ are defined in the same way as in eq. (9). The values calculated supposing $p = 0$ and $q\hbar = p_F$. For subband electrons $q \simeq (3N_{se}\pi^2)^{1/3}$ in the case i or $q \simeq (3N_{se}\pi^2/2 + k_m^3)^{1/3} - k_m$ in the case ii (see final part of Sec. I and Fig. 1). The results of our calculation one can see in Fig. 2. The difference between $|eR_H|^{-1}$ and concentration is very small because of strong nonparabolicity of subband. The latter not only affects on dynamic properties of electrons, but also essentially decrease the relaxation times [see eqs. (9)-(11)]. The subband transport is maximally effective when the width of subband is maximal and it is about half filled [compare line 3 in Fig. 1(b,c) and line 3 in Fig. 2(b) below $T = 100\ K$]. As far as $\lambda \propto 1/\sqrt{T}$ (approximately) Mott transition appears in low temperature region for lower doping levels in comparison with high temperature region. Discussing the region near the Mott transition, we have to emphasize, that the closer system to the Mott transition the closer the donor

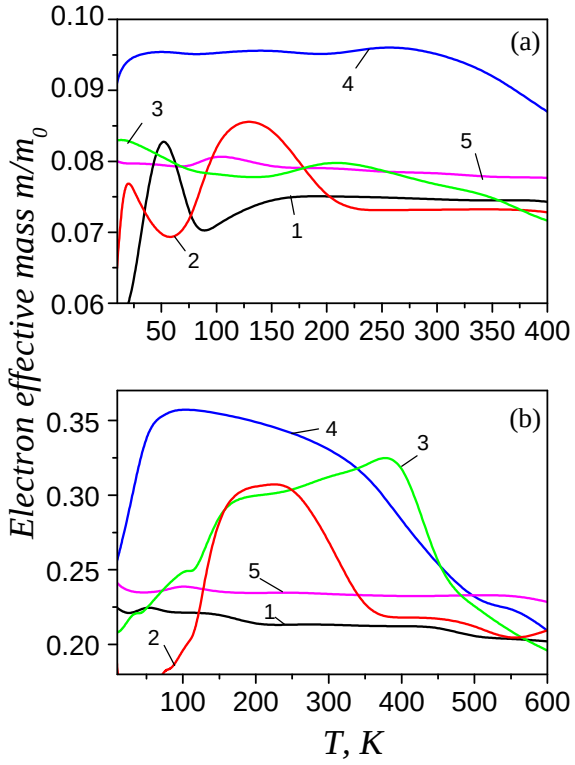

FIG. 4. Renormalized electron effective mass of GaAs (a) and GaN (b) as functions of temperature. The calculation was performed for different doping levels. (a) lines 1, 2, 3, 4, 5 correspond to the doping levels $N_d = 10^{15},\ 10^{16},\ 10^{17},\ 10^{18},\ 10^{19}$ cm^{-3}. (b) lines 1, 2, 3, 4, 5 correspond to the doping levels $N_d = 10^{16},\ 10^{17},\ 10^{18},\ 10^{19},\ 10^{20}$ cm^{-3}.

subband to the bottom of the conduction band. In thus intermediate region conduction band electron concentration increases with decreasing of the temperature. The theoretical results is in a good agreement with experimental data for GaN [see Fig. 2 (b)], and also they are corroborated with the experimental measurements in GaAs [compare Fig. 2(a) lines 1–4 at $T \lesssim 15\ K$ and results from Refs. 6 and 8 for $N_d \simeq 3.5 \times 10^{16}\ cm^{-3}$].

The results of effective masses calculation are presented in Fig. 4(a,b). The electron effective masses are mostly determined by the electron-electron exchange interaction and electron-optical phonon interaction. The latter is dependent on dopant concentration because of dynamical screening $\propto |\epsilon_e|^{-2}$. This function is maximal when $\omega = \Omega_p$ and $\overline{v}q \ll \omega$. Therefore, maximal renormalization of electron masses correspond to the doping levels $N_d \simeq 10^{18}$ cm^{-3} for GaAs and $N_d \simeq 10^{19}\ cm^{-3}$ for GaN. The further increasing of doping levels leads to the fast decreasing of renormalization effect because the all impotent q in eq. (15) satisfies $\overline{v}q \gtrsim \omega$ now. In GaAs this effect of dynamic screening can not be implemented because of stronger nonparabolicity of conduction band. The frequencies which are relevant for dynamical screening of optical phonon one can find in Fig. 3.

The light hole and heavy hole renormalization energies are different. Therefore, heavy doping leads to removal of degeneracy at the Γ-point of valence band. The corresponding values of valence bands splitting $(\Sigma^{hh} - \Sigma^{lh})\big|_{p=0}$ are presented in Fig. 5(a,b).

The results of bandgap narrowing calculation are presented in Fig. 6. Notice, that in low temperature region optical phonons affect only on the top of valence band only. Thus optical phonon influence is clearly observed on the experimental data from Ref. 21 [Fig. 6(a)].

V. CONCLUSIONS

We considered energy renormalization and Mott transition in n-GaAs and n-GaN. In general, the problems are very complicated. Therefore, we realized approaches that have low precision in a special region of parameters. To illustrate, the parameter $r_B \gg N_d^{-1/3}$ near the Mott transition that is incorrect. In addition, eq. (5) not valid

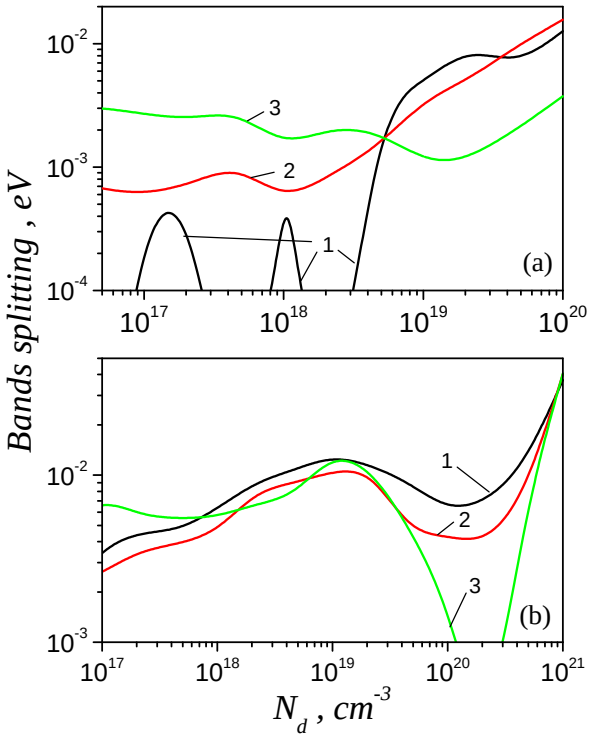

FIG. 5. Splitting of the light hole and heavy hole bands of GaAs (a) and GaN (b) as the functions of dopant concentration N_d. The lines 1–3 correspond to different temperatures $T = 4$, 77, 300 k.

if the electron concentration in the conduction band is much lower than N_d, because we take into account donors potential only. More over, formula (16) for the inverse screening length λ is incorrect in low temperature limit $T \to 0$. Therefore, the calculations performed for $T \lesssim 10\ K$ are questionable. We have restricted the self-energy series by the second term in eq. (8) which is conventional approach. On the other hand, we have used averaged Green's functions with renormalized effective mass and non-zero imaginary part of self-energy. This is supposed to essentially improve precision. We used renormalized effective mass to calculate the donor subband energy dispersion law. The assumption is justified because autocorrelation lengths of considered perturbations $l_{\alpha-e,d,opt} \ll r_B$. The averaging procedures in eqs. (10) and (12) is justified because the main contribution to the corresponding terms in eq. (8) comes from the region, where $\varepsilon(\Delta\mathbf{p}) \gg \varepsilon^{im}(\Delta\mathbf{p})$ and $\varepsilon(\mathbf{p}_2 + \Delta\mathbf{p}) - \varepsilon(\mathbf{p}_2) \sim \Delta p^2/2m$. We also omitted consideration of the interband transitions and subband-conduction band transitions. Such assumption needs additional investigation.

Nevertheless, the results obtained are in good agreement with different experimental works [2, 3, 6–9, 20, 21]. Below, we enumerate the main theoretical results. The Mott transition is defined by the condition $\lambda r_{B0} \simeq 0.83$. Where the Bohr radius r_{B0} and the inverse screening length λ being calculated with allowance made for renormalized effective mass m. The mass renormalization is strongly affected by the dynamically screened optical phonons. Because of the dynamic screening, the masses of n-GaAs and n-GaN are maximally renormalized if their doping levels are $N_d \simeq 10^{18}$ and $N_d \simeq 10^{19}\ cm^{-3}$ correspondingly. For higher doping levels the renormalization effect is lower, because Maxwell relaxation times become too short. The bandgap narrowing is also strongly affected by the dynamically screened optical phonons, especially near the doping levels mentioned above.

Finally, we enumerate the basic parameters values used in our numerical calculations: the effective masses for intrinsic semiconductors are $m = 0.067m_0$, $m_{lh} = -0.082m_0$, $m_{hh} = -0.51m_0$ for GaAs and $m = 0.2m_0$, $m_{lh} = -0.3m_0$, $m_{hh} = -0.8m_0$ for GaN; static dielectric constants are $\epsilon = 12.9$ and $\epsilon = 8.9$, high frequency dielectric constants are $\epsilon_\infty = 10.9$ and $\epsilon_\infty = 6$, optical phonon energies are $\hbar\omega_o = 36\ meV$ and $\hbar\omega_o = 85\ meV$ for GaAs and GaN correspondingly.

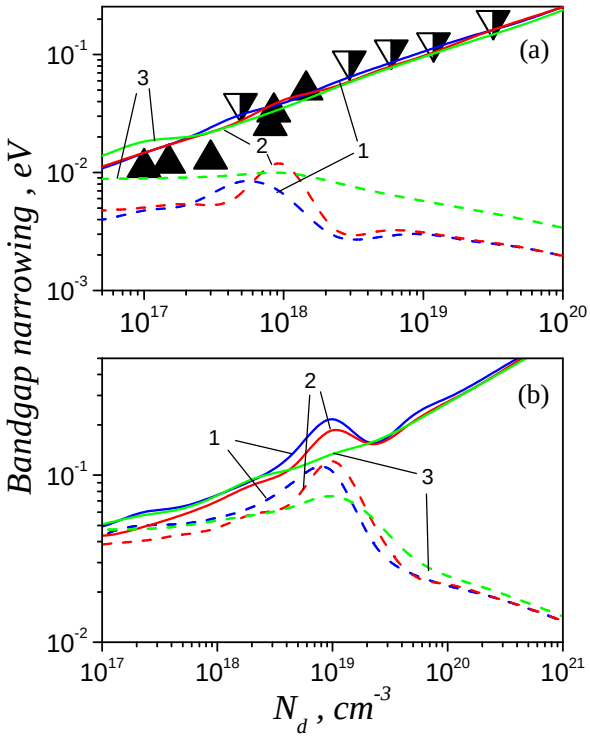

FIG. 6. The bandgap narrowing of GaAs (a) and GaN (b) as the functions of doping level (solid lines). The dashed lines take into account optical phonons effect only. The lines 1, 2, 3 correspond to the temperatures $T = 4$, 77, 300 K. The experimental data sets are extracted from Refs. 20 and 21.

Appendix A: Dynamic screening

When considering virtual transitions in eq. (8) the charge screening is very essential. High frequency perturbations $V(k,\omega) \propto \exp(i\mathbf{kr} - i\omega t)$ may involve plasmon excitation processes. If perturbation frequency ω is on the order of plasmon frequency Ω_p and much larger than other characteristic frequencies of the system then plasmon pole model works very well. If the system is relaxing to the equilibrium during $\tau < \omega^{-1}$, then plasmon excitation becomes inefficient and one has to obtain the usual statically screened potential $V(k,\omega) \propto (k^2 + \lambda^2)^{-1}$. In addition, the plasmon pole model may be incorrect in the short-wave limit $kp_F/m \sim \omega$ because in generally plasmon resonant excitation is k-dependent. The problem is to obtain a dynamic screening model that may be extrapolated to any values of k and ω. We start from the linearized kinetic equation

$$\frac{\partial \delta f_{\mathbf{r},t}}{\partial t} + e\mathbf{E}_{\mathbf{r},t}\frac{\partial f_{\varepsilon(p)}}{\partial \mathbf{p}} + \frac{\partial \varepsilon(p)}{\partial \mathbf{p}}\frac{\partial \delta f_{\mathbf{r},t}}{\partial \mathbf{r}} = -\delta f_{\mathbf{r},t}/\tau \tag{A1}$$

where $f_{\varepsilon(p)}$ is the Fermi distribution function, the perturbation induced part $\delta f_{\mathbf{r},t} \propto \exp(i\mathbf{kr})$ of distribution, and the field $\mathbf{E}_{\mathbf{r},t} = [\mathbf{E}^0 \exp(-i\omega t) + \mathbf{E}^l_t] \exp(i\mathbf{kr})$ which includes initial perturbation field $\propto \mathbf{E}^0 \exp(-i\omega t)$ and field induced by plasma oscillation $\propto \mathbf{E}^l_t$. For simplicity we suppose that relaxation time $\tau = \tau_d$.

It is easy to obtain equation of longitudinal oscillations using the Maxwell equation $\nabla[\mathbf{E}^l_t \exp(i\mathbf{kr})] = 4\pi\rho_{\mathbf{r},t}/\epsilon$ and continuity equation $\nabla \mathbf{J}_{\mathbf{r},t} = -\dot{\rho}_{\mathbf{r},t}$:

$$\frac{d^2\mathbf{E}^l_t}{dt^2} = -\frac{4\pi}{\epsilon}\frac{d\mathbf{j}_t}{dt} \tag{A2}$$

where $\mathbf{j}_t = \mathbf{J}_{\mathbf{r},t} \exp(-i\mathbf{kr})$. The current is defined by perturbation induced part of distribution

$$\mathbf{j}_t = \frac{2e^2}{3}\int \frac{d^3\mathbf{p}}{(2\pi\hbar)^3}\left(\frac{\partial \varepsilon(p)}{\partial p}\right)^2 \frac{\partial f_\varepsilon}{\partial \varepsilon}\int_0^t dt' \exp\left[-\left(\nu + i\mathbf{k}\frac{\partial \varepsilon(p)}{\partial \mathbf{p}}\right)(t-t')\right][\mathbf{E}^0 \exp(-i\omega t') + \mathbf{E}^l_{t'}]. \tag{A3}$$

Next, we replace the integrant factor $\int_{-1}^{1} d\chi \, \exp[ik(\partial\varepsilon/\partial p)\chi(t-t')]$ by the factor $\int_{-1}^{1} d\chi \, \exp[ik\overline{v}\chi(t-t')]$, where

$$\overline{v} = -\frac{\int_0^\infty d\varepsilon\rho(\varepsilon)\left(\frac{\partial\varepsilon(p)}{\partial p}\right)^3 \frac{\partial f_\varepsilon}{\partial\varepsilon}}{\int_0^\infty d\varepsilon\rho(\varepsilon)\left(\frac{\partial\varepsilon(p)}{\partial p}\right)^2 \frac{\partial f_\varepsilon}{\partial\varepsilon}}. \tag{A4}$$

Then substituting (A3) to (A2) one can obtain equation of longitudinal oscillation:

$$\frac{d\mathbf{E}_t^l}{dt} = \Omega_p^2 \int_0^t dt' [\mathbf{E}^0 \exp(-i\omega t') + \mathbf{E}_{t'}^l] \int_{-1}^{1} d\chi \exp[ik\overline{v}\chi(t-t')], \tag{A5}$$

where we denote

$$\Omega_p^2 = \frac{4\pi e^2}{\epsilon} \int_0^\infty d\varepsilon\rho(\varepsilon) \frac{\partial^2\varepsilon}{\partial\mathbf{p}^2} f_\varepsilon. \tag{A6}$$

The dynamic screening is defined by the ratio $(E^0 + E^l_{t\to\infty})/E^0$. But the plasma oscillations appear only if $\tau\omega > 1$. Otherwise we suppose static screening. The final result is:

$$\epsilon_e^{-1}(k,\omega) \simeq \begin{cases} 1 + \frac{\Omega_p^2}{2k\overline{v}} \ln\left(\frac{\omega+k\overline{v}+i\tau^{-1}}{\omega-k\overline{v}+i\tau^{-1}}\right) / \left[\omega - \frac{\Omega_p^2}{2k\overline{v}} \ln\left(\frac{\omega+k\overline{v}+i\tau^{-1}}{\omega-k\overline{v}+i\tau^{-1}}\right)\right], & \tau\omega > 1; \\ \frac{k^2}{k^2+\lambda^2}, & \tau\omega < 1. \end{cases} \tag{A7}$$

REFERENCES

[1] J P Silvera and F Briones 1994 Appl. Phys. Lett **65** (5), 573
[2] Leonard J Brillson 1993 *Contacts to Semiconductors. Fundamental technology* Noyes Publications, New Jersey
[3] Ф П Касаманлы и Д Н Наследова 1973 *Арсенид галлия. Получение, свойства и применение* Москва
[4] N F Mott 1949 Proc. Phys. Soc. (London) A **62**, 416
[5] G L 1949 Pearson and Bardeen, Phys. Rev. **75** (5), 865
[6] G E Stillman, C M Wolfe and J O Dimmock 1970 J. Chem. Solids **31** 1199
[7] W Götz and N M Johnson, C Chen, H Liu, C Kuo, and W Imler 1996 Appl. Phys. Lett. **68** (22), 3144
[8] M Benzaquen, D Walsh, and K Mazuruk 1987 Phys. Rev. B **75** (9), 4748
[9] Z Bougrioua, J-L Farvacque, I Moerman, P Demeester, J J Harris, K Lee, G van Tendeloo, O Lebedev, and E J Thrush 1999 Phys. Stat. Sol. (b) **216**, 571
[10] A Amo, M D Marthin, and L Vina, A I Toropov and K S Zhuravlev 2007 Appl. Phys. Lett. **101** (8), 081717
[11] L D Landau, E M Lifshitz 1958 *Quantum Mechanics: Non-relativistic Theory*, Pergamon Press
[12] J Luttinger, W Kohn 1955 Phys. Rev. **97**, 869
[13] I M Tsidilkovski 1982 *Band structure of semiconductors*, Oxford, Eng. (translated by R.S. Wadhwa); New York: Pergamon Press
[14] A Selloni and S T Pantelides 1982 Phys. Rev. Lett. **49** 586
[15] K-F Berggren and B. Sernelius 1984 Phys. Rev B **29** (10), 5575
[16] A I Anselm 1982 *Introduction to the theory of semiconductors*, Publisher: Prentice Hall Professional Technical Reference
[17] F M Abou El-Ela and A Z Mohamed 2013 Appl. Phys. Res. **5** (2)
[18] K-F Berggren and B E Sernelius 1981 Phys. Rev. B **24**, (4) 1971
[19] B E Sernelius 1986 Phys. Rev. B **33**, (12) 8582
[20] Huade Yao and A Compaan 1990 Appl. Phys. Lett. **57**, (2) 147
[21] M K Hudait, P Modak, S B Krupanidhi 1999 Materials Science and Engineering B **60**, 1
[22] Fedir T. Vasko, Oleg E. Raichev 2005 *Quantum kinetic theory and applications* Springer, New York Science